53rd AIAA/ASME/ASCE/AHS/ASC Structures, Structural Dynamics and Materials Conference
20th AI
23 - 26 April 2012, Honolulu, Hawaii

AIAA 2012-1369

Application of Quasi-Homogeneous Anisotropic Laminates in Grid-stiffened Panel Design

C. B. York*
University of Glasgow, Glasgow, Scotland, G12 8QQ

D. Kennedy†
Cardiff University, Cardiff, Wales, CF24 3AA

Composite laminates are derived for standard configurations with quasi-homogeneous anisotropic properties, whereby in-plane and out-of-plane stiffness properties are concomitant. Dimensionless parameters, and their relationship to the well-known ply-orientation-dependent lamination parameters, are also developed from which the elements of the extensional and bending stiffness matrices are readily calculated for any fiber/resin properties. The definitive list of laminate configurations for up to 21 plies is presented, together with graphical representations of the lamination parameter design space for standard ply orientations ±45, 0 and 90°. Finally, the potential of quasi-homogeneous anisotropic laminates as an optimum design solution for anisogid structures is explored for cases where buckling and strength constraints are both active.

Nomenclature

a,b	=	Length and width of each repeating bay.
$\mathbf{A}$,A_{ij}	=	extensional (membrane) stiffness matrix and its elements (i,j = 1, 2, 6).
$\mathbf{B}$,B_{ij}	=	bending-extension-coupling stiffness matrix and its elements (i,j = 1, 2, 6).
$\mathbf{D}$,D_{ij}	=	bending (flexural) stiffness matrix and its elements (i,j = 1, 2, 6).
E_1,E_2	=	Young's moduli parallel to and normal to fibre direction.
G_{12}	=	in-plane shear modulus.
H	=	laminate thickness (= $n \times t$).
k	=	ply number.
n	=	number of plies in laminate stacking sequence.
$n_{\pm}$,$n_{\square}$,$n_{\bullet}$	=	membrane stiffness parameters for angle-ply and cross-ply sub-sequences.
$\mathbf{N}$	=	in-plane force resultants (= $\{N_x,N_y,N_{xy}\}^T$).
N_x,N_y	=	in-plane axial load per unit length.
N_{xy}	=	in-plane shear flow.
$\mathbf{M}$	=	out-of-plane moment resultants (= $\{M_x,M_y,M_{xy}\}^T$).
M_x,M_y	=	bending moments per unit length about principal axes.
M_{xy}	=	twist moment per unit length.
Q_{ij}	=	reduced stiffness (i,j = 1, 2, 6).
Q'_{ij}	=	transformed reduced stiffness (i,j = 1, 2, 6).
t	=	ply thickness.
U_i	=	laminate invariants (i=1,2,…,5).
x,y,z	=	principal axes.
α	=	skew angle.
γ_{xy}	=	in-plane shear strain.
$\boldsymbol{\varepsilon}$	=	in-plane strains (= $\{\varepsilon_x,\varepsilon_y,\gamma_{xy}\}^T$).

---

* Senior Lecturer, School of Engineering.

† Professor, School of Engineering. Senior Member, AIAA.

$\varepsilon_x,\varepsilon_y$	=	in-plane axial strains.
$\boldsymbol{\kappa}$	=	curvatures (= $\{\kappa_x,\kappa_y,\kappa_{xy}\}^T$).
κ_x,κ_y	=	curvatures about principal axes.
κ_{xy}	=	twist curvature.
$\xi_{1\text{-}4}$	=	lamination parameters for extensional stiffness (ξ_1,ξ_2,ξ_3,ξ_4).
$\xi_{9\text{-}12}$	=	lamination parameters for bending stiffness ($\xi_9,\xi_{10},\xi_{11},\xi_{12}$).
χ	=	phase shift across adjacent bays.
$\zeta,\zeta_{\pm},\zeta_{\cap},\zeta_{\blacktriangle}$	=	bending stiffness parameters for laminate, and angle-ply and cross-ply sub-sequences.
$+,-,\pm$	=	angle plies, used in stacking sequence definition.
$\mathrm{O},\bullet$	=	cross-plies, used in stacking sequence definition.

Keywords

Quasi-Homogeneous, Anisogrid, Optimization, Buckling, Strength Constraints.

I. Introduction

A Quasi-Homogeneous Anisotropic Laminate, or QHAL, is described[1] as having identical anisotropy with respect to both extension and bending, providing maximum (and minimum) in-plane and out-of-plane reinforcement in the same direction, and thus providing a minimum mass solution. The extensional and bending stiffness properties of a QHAL may therefore be described as concomitant and as such, represent a simplification in design, since only the extensional stiffness properties need to be calculated. However, to provide a minimum mass solution implies that the extensional stiffness properties satisfy the material strength constraints in the same way that the bending stiffness properties satisfy the buckling constraints, where the latter is strongly influenced by the planform geometry.

It is logical to suppose that the optimum buckling solution for a rectangular plate arises from a fully uncoupled orthotropic laminate, since anisotropy in bending, or more correctly bending-twisting coupling, which generally occurs in balanced and symmetric designs, is known to reduce the compression buckling strength. Equally, the same rectangular plate is better served by an unbalanced laminate if subject only to pure shear loading. However, skew planform geometry would provide a similar buckling strength advantage without requiring a change in laminate design. The optimum solution is less apparent for multiple load cases and the question must be raised as to whether optimized solutions, satisfying buckling and strength constraints simultaneously, arise from Quasi-Homogeneous Anisotropic Laminates.

To investigate such a hypothesis, this study will focus on the initial buckling response of continuous composite plate arrays, subject to material strength constraints, to assess the potential of quasi-homogeneous anisotropic laminates as an optimum design solution for a range of planform configurations, including isogrid and orthogrid, together with more general configurations, termed anisogrid.

Figure 1 illustrates typical planform geometries, i.e. a rectangular array of supports, simulating an orthogrid panel and anisogrid panels, used to describe hexagonal or skew planform geometries. An offset isogrid configuration is also considered, but not shown, which arises because of practical manufacturing considerations, to reduce the number of overlapping plies at stiffener intersections, thus reducing the likelihood of stiffener separation from delamination propagation which is often initiated at these sites. Increasing this offset gives rise to the eccentric isogrid variant or anisogrid, whereby the orthogonal, or x-axis aligned support is positioned along the centre-line of the bay. The planform geometry now consists of adjacent triangular and hexagonal cells.

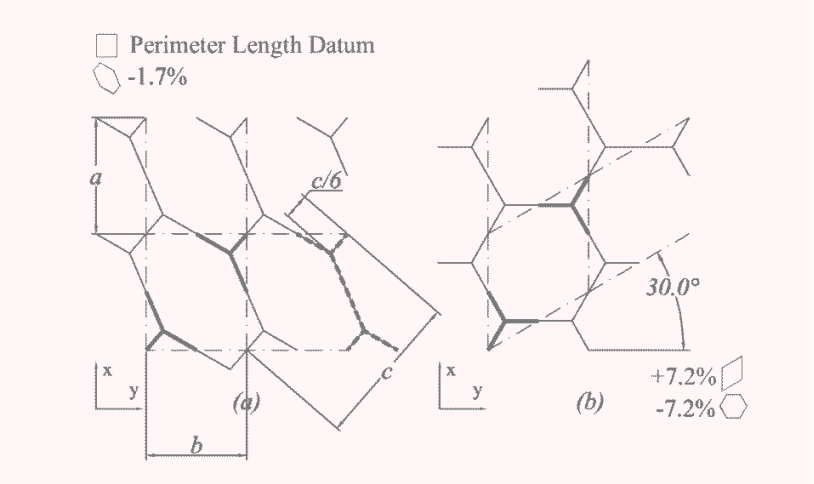

Figure 1 – Example grid stiffened panel array geometries (*after Ref. 3*) with equivalent planform area (aspect ratio $a/b = 1.15$) for (a) rectangular (orthogrid) and hexagonal (anisogrid); (b) skew and regular hexagonal. The percentage increase in perimeter length, above the rectangular datum, is indicated alongside thumbnail sketches of each planform shape.

The outcomes of this study form, in part, an extension to a previous investigation of buckling interaction for metallic[2] and fully uncoupled laminate[3] panel structures. As in the previous work, configurations representing anisogrid panel arrays are again a primary focus of the investigation, having been shown to possess significant buckling strength advantages over the more common square planform. These configurations also have a net reduction in panel weight due to the use of novel support configurations, which gives rise to a reduction in the length of the supporting perimeter. The stiffeners are modeled as rigid point supports with rotational freedom so that effects on plate buckling behavior resulting from the continuous nature of the plate can be studied independently of the bending and torsional interactions, which normally arise from the supporting stiffeners. Results will demonstrate the relative increase in buckling strength between laminates with concomitant and non-concomitant properties, where concomitant anisotropic properties implies matching shear-extension and bending-twisting coupling and laminates with these matching properties are generally referred to as Quasi-Homogeneous Anisotropic Laminates[1]. Fully isotropic laminate configurations are employed as a benchmark case[4] to highlight the combined effects of shear-extension and bending-twisting coupling. The effect of uncoupled, Quasi-Homogeneous Orthotropic Laminates[4] will also be considered in order to isolate the effects of anisotropy on the concomitant properties.

II. Characterization of Laminated Composite Material

Composite laminates are typically characterized in terms of their response to mechanical (and/or thermal) loading, which is generally associated with a description of the coupling behavior, unique to this type of material. The well-known **ABD** relation from classical lamination theory is often expressed using compact notation:

$$\begin{Bmatrix} \mathbf{N} \\ \mathbf{M} \end{Bmatrix} = \begin{bmatrix} \mathbf{A} & \mathbf{B} \\ \mathbf{B} & \mathbf{D} \end{bmatrix} \begin{Bmatrix} \boldsymbol{\varepsilon} \\ \boldsymbol{\kappa} \end{Bmatrix} \tag{1}$$

The coupling behavior, which is dependent on the form of the elements in each of the extensional (**A**), coupling (**B**) and bending (**D**) stiffness matrices, is conveniently described by an extended subscript notation, defined previously in an Engineering Sciences Data Unit (ESDU) data item[5]. Here, a balanced and symmetric stacking sequence, which generally possesses bending anisotropy, gives rise to coupling between bending and twisting and are referred to by the designation $\mathbf{A}_S\mathbf{B}_0\mathbf{D}_F$, signifying that the elements of the extensional stiffness matrix ($\mathbf{A}_S$) have the Simple, uncoupled form:

$$\begin{bmatrix} A_{11} & A_{12} & 0 \\ & A_{22} & 0 \\ \text{Sym.} & & A_{66} \end{bmatrix} \tag{2}$$

The bending-extension coupling matrix ($\mathbf{B}_0$) is null, i.e. no coupling between in-plane and out-of-plane responses, whilst all elements of the bending stiffness matrix ($\mathbf{D}_F$) are Finite, and have the form:

$$\begin{bmatrix} D_{11} & D_{12} & D_{16} \\ & D_{22} & D_{26} \\ \text{Sym.} & & D_{66} \end{bmatrix} \tag{3}$$

The laminates investigated in this study possess both in-plane coupling, i.e. between the shear force resultant (N_{xy}) and extensional strains (ε_x, ε_y), i.e. $A_{16} = A_{26} \neq 0$, and out-of-plane coupling, i.e. between moment resultants (M_x, M_y) and twist curvature (κ_{xy}), i.e. $D_{16} = D_{26} \neq 0$.

It is clear from the literature[6,7] that the extensional (**A**) and bending (**D**) stiffness matrices possess one of two forms: either fully uncoupled ($\mathbf{A}_S$, $\mathbf{D}_S$) or fully coupled ($\mathbf{A}_F$, $\mathbf{D}_F$). The isotropic form of these matrices, where $\mathbf{D}_I$ and/or $\mathbf{A}_I$ replace $\mathbf{D}_S$ and/or $\mathbf{A}_S$ respectively, are excluded because they have been shown[4] to represent subsets of the specially orthotropic (uncoupled) form. An additional subset[4] includes laminates for which the elements of the bending stiffness matrix are related directly to those of the extensional stiffness matrix and the laminate thickness, H by:

$$D_{ij} = A_{ij}H^2/12 \tag{4}$$

This subset represents a significant simplification in design, and for the uncoupled form ($\mathbf{A}_S$, $\mathbf{D}_S$) can be described as a Quasi-Homogeneous Orthotropic Laminate, or **QHOL**, providing identical orthotropy with respect to both extension and bending, thus providing maximum (and minimum) in-plane and out-of-plane reinforcement in the same direction. The coupled form ($\mathbf{A}_F$, $\mathbf{D}_F$), which is the primary focus of the current article, has been described elsewhere[1] as a Quasi-Homogeneous Anisotropic Laminate, or **QHAL**, possessing identical anisotropy with respect to both extension and bending, i.e. shear-extension and bending-twisting coupling. It has also been described as representing an optimum design solution due to the concomitant properties, which provide the maximum reinforcement in same direction for both extension and bending. This hypothesis has, however, yet to be proven.

The illustrations presented in Fig. 2 represent the thermal (contraction) response of four families of laminates that remain flat following a typical elevated temperature curing process. The $\mathbf{A}_F\mathbf{B}_0\mathbf{D}_F$ designation represents the family of laminates from which quasi-homogeneous configurations are sought; and the laminate stacking sequences presented are merely representative examples from the minimum ply number grouping for each designation. A response-based labeling is used in the caption, but is complementary to the subscript labeling system used above, which builds on the Engineering Sciences Data Unit subscript notation[5]. The fully uncoupled form ($\mathbf{A}_S\mathbf{B}_0\mathbf{D}_S$) is described as a *Simple* laminate, whereas the coupled forms are described in terms of the response that the laminate exhibits to various combination of force and moment resultants, using a *cause* and *effect* relationship. A laminate is therefore described as an *E-S* laminate if *Extension* (*E*) causes a *Shearing* (*S*) effect, whereas if *Bending* causes a *Twisting* effect then the laminate is described as a *B-T* laminate. Note that each *cause* and *effect* pair is underlined.

The *cause* and *effect* labeling used in the caption to Fig. 2 describes the coupling relationship between an applied (bending and/or twisting) moment resultant and the associated extensional (and/or shearing) strains, whereas Table 1 describes the coupling relationship between an applied (axial and/or shear and/or thermal) force resultant and the associated curvatures (and/or twist-curvature) for an unrestrained plate. Each pair of *cause* and *effect* descriptors of the response-based labeling is therefore reversible.

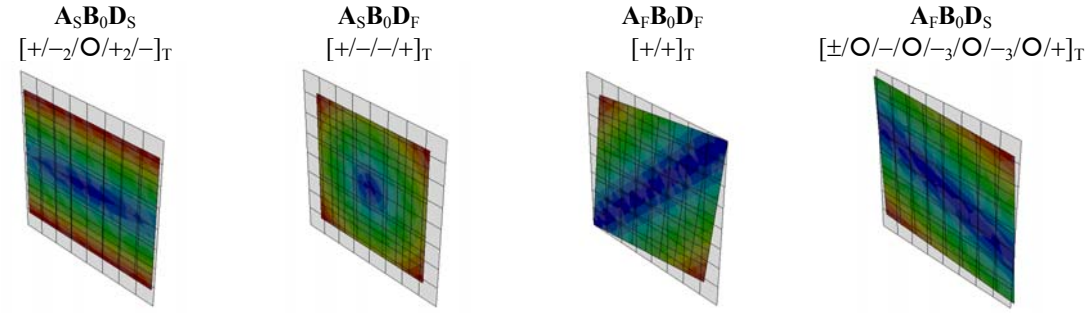

Figure 2 – Coupling responses, due to free thermal contraction, for the: ($\mathbf{A_S B_0 D_S}$) *Simple* laminate; ($\mathbf{A_S B_0 D_F}$) *B-T* laminates with bending-twisting coupling; ($\mathbf{A_F B_0 D_F}$) *E-S*;*B-T* laminates with extension-shearing and bending-twisting coupling and; ($\mathbf{A_F B_0 D_S}$) *E-S* laminates with extension-shearing coupling. Displacement magnitudes are not to scale.

Table 1 – Response based labeling with associated form of matrix for: (a) extensional stiffness and; (b) bending stiffness. Compact notation subscripts, corresponding to specific form of stiffness matrices, are summarized in the table footnotes.

(a)

Compact notation (*after Ref. 5*)	Response-based labeling	Matrix form
$\mathbf{A_S}$	Simple laminate	$\begin{bmatrix} A_{11} & A_{12} & 0 \\ A_{21} & A_{22} & 0 \\ 0 & 0 & A_{66} \end{bmatrix}$
$\mathbf{A_F}$	Shear-Extension; *S-E*	$\begin{bmatrix} A_{11} & A_{12} & A_{16} \\ A_{21} & A_{22} & A_{26} \\ A_{61} & A_{62} & A_{66} \end{bmatrix}$

(b)

Compact notation (*after Ref. 5*)	Response-based labeling	Matrix form
$\mathbf{D_S}$	Simple laminate	$\begin{bmatrix} D_{11} & D_{12} & 0 \\ D_{21} & D_{22} & 0 \\ 0 & 0 & D_{66} \end{bmatrix}$
$\mathbf{D_F}$	Twisting-Bending; *T-B*	$\begin{bmatrix} D_{11} & D_{12} & D_{16} \\ D_{21} & D_{22} & D_{26} \\ D_{61} & D_{62} & D_{66} \end{bmatrix}$

Summary of Matrix sub-scripts for compact notation

0 = All elements (of stiffness matrix) zero.
F = All elements Finite.
S = Specially orthotropic (uncoupled or Simple) form.

III. Calculation of extensional, coupling and bending stiffness terms

The calculation procedure for the elements (A_{ij} and D_{ij}) of the extensional (**A**) and bending (**D**) stiffness matrices, using the dimensionless parameters provided in the appendix, are as follows:

$$A_{ij} = \{n_{\pm}(n_{+}/n_{\pm})Q'_{ij+} + n_{\pm}(1 - n_{+}/n_{\pm})Q'_{ij-} + n_{\mathbf{O}}Q'_{ij\mathbf{O}} + n_{\bullet}Q'_{ij\bullet}\} \times t \tag{5}$$

$$D_{ij} = \{\zeta_{\pm}/2 \times Q'_{ij+} + \zeta_{\pm}/2 \times Q'_{ij-} + \zeta_{\mathbf{O}}Q'_{ij\mathbf{O}} + \zeta_{\bullet}Q'_{ij\bullet}\} \times t^3/12 \tag{6}$$

noting that all laminates have zero coupling stiffness matrix (**B** = **0**) in this study.

The form of Eq. (6) was developed for the Simple (uncoupled) form of the bending stiffness matrix but is readily modified to account for the presence of bending-twisting coupling by replacing $\zeta_{\pm}/2 \times Q'_{ij+}$ with $\zeta_{\pm}\,(\zeta_{+}/\zeta_{\pm}) \times Q'_{ij+}$ or $\zeta_{+} \times Q'_{ij+}$, and $\zeta_{\pm}/2 \times Q'_{ij-}$ with $\zeta_{\pm}(1 - \zeta_{+}/\zeta_{\pm}) \times Q'_{ij-}$, or $\zeta_{-} \times Q'_{ij-}$.

$$D_{ij} = \{\zeta_{\pm}\,(\zeta_{+}/\zeta_{\pm}) \times Q'_{ij+} + \zeta_{\pm}(1 - \zeta_{+}/\zeta_{\pm}) \times Q'_{ij-} + \zeta_{\circ} Q'_{ij\circ} + \zeta_{\bullet} Q'_{ij\bullet}\} \times t^3/12 \tag{7}$$

The use of this modified equation requires the calculation of an additional stiffness parameter, ζ_{+}, relating to the bending stiffness contribution of positive (θ) angle plies. However, for quasi-homogeneous anisotropic laminates, Eqs (6) or (7) may be replaced by Eq. (4).

The transformed reduced stiffness terms in Eqs (5) and (6) are given by:

$$Q'_{11} = Q_{11}\cos^4\theta + 2(Q_{12} + 2Q_{66})\cos^2\theta\sin^2\theta + Q_{22}\sin^4\theta$$

$$Q'_{12} = Q'_{21} = (Q_{11} + Q_{22} - 4Q_{66})\cos^2\theta\sin^2\theta + Q_{12}(\cos^4\theta + \sin^4\theta)$$

$$Q'_{16} = Q'_{61} = \{(Q_{11} - Q_{12} - 2Q_{66})\cos^2\theta + (Q_{12} - Q_{22} + 2Q_{66})\sin^2\theta\}\cos\theta\sin\theta$$

$$Q'_{22} = Q_{11}\sin^4\theta + 2(Q_{12} + 2Q_{66})\cos^2\theta\sin^2\theta + Q_{22}\cos^4\theta$$

$$Q'_{26} = Q'_{62} = \{(Q_{11} - Q_{12} - 2Q_{66})\sin^2\theta + (Q_{12} - Q_{22} + 2Q_{66})\cos^2\theta\}\cos\theta\sin\theta$$

$$Q'_{66} = (Q_{11} + Q_{22} - 2Q_{12} - 2Q_{66})\cos^2\theta\sin^2\theta + Q_{66}(\cos^4\theta + \sin^4\theta) \tag{8}$$

and the reduced stiffness terms by:

$$Q_{11} = E_1/(1 - \nu_{12}\nu_{21})$$

$$Q_{12} = \nu_{12}E_2/(1 - \nu_{12}\nu_{21}) = \nu_{21}E_1/(1 - \nu_{12}\nu_{21})$$

$$Q_{22} = E_2/(1 - \nu_{12}\nu_{21})$$

$$Q_{66} = G_{12} \tag{9}$$

For optimum design of angle ply laminates, lamination parameters are often preferred, since these allow the stiffness terms to be expressed as linear variables. The optimized lamination parameters may then be matched against a corresponding set of laminate stacking sequences. In the context of the quasi-homogeneous anisotropic laminates presented in the current article, only 4 lamination parameters are required and are related through the following expressions:

$$\xi_1\,(=\xi_9) = \{n_{\pm}(n_{+}/n_{\pm})\cos(2\theta_{+}) + n_{\pm}(1 - n_{+}/n_{\pm})\cos(2\theta_{-}) + n_{\circ}\cos(2\theta_{\circ}) + n_{\bullet}\cos(2\theta_{\bullet})\}/n$$

$$\xi_2\,(=\xi_{10}) = \{n_{\pm}(n_{+}/n_{\pm})\cos(4\theta_{+}) + n_{\pm}(1 - n_{+}/n_{\pm})\cos(4\theta_{-}) + n_{\circ}\cos(4\theta_{\circ}) + n_{\bullet}\cos(4\theta_{\bullet})\}/n$$

$$\xi_3\,(=\xi_{11}) = \{n_{\pm}(n_{+}/n_{\pm})\sin(2\theta_{+}) + n_{\pm}(1 - n_{+}/n_{\pm})\sin(2\theta_{-}) + n_{\circ}\sin(2\theta_{\circ}) + n_{\bullet}\sin(2\theta_{\bullet})\}/n$$

$$\xi_4\,(=\xi_{12}) = \{n_{\pm}(n_{+}/n_{\pm})\sin(4\theta_{+}) + n_{\pm}(1 - n_{+}/n_{\pm})\sin(4\theta_{-}) + n_{\circ}\sin(4\theta_{\circ}) + n_{\bullet}\sin(4\theta_{\bullet})\}/n \tag{10}$$

Note that for laminates consisting of standard ply angle orientations, i.e. +45, -45, 0 and 90°, only 3 lamination parameters are required, since $\xi_4 = 0$, and the extent of this 3-dimensional lamination parameter design space can be readily illustrated.

For non-homogeneous properties, a further 4 lamination parameters are also required:

$$\xi_9 = \{\zeta_{\pm}(\zeta_{+}/\zeta_{\pm})\cos(2\theta_{+}) + \zeta_{\pm}(1 - \zeta_{+}/\zeta_{\pm})\cos(2\theta_{-}) + \zeta_{\circ}\cos(2\theta_{\circ}) + \zeta_{\bullet}\cos(2\theta_{\bullet})\}/\zeta$$

$$\xi_{10} = \{\zeta_{\pm}(\zeta_{+}/\zeta_{\pm})\cos(4\theta_{+}) + \zeta_{\pm}(1 - \zeta_{+}/\zeta_{\pm})\cos(4\theta_{-}) + \zeta_{\circ}\cos(4\theta_{\circ}) + \zeta_{\bullet}\cos(4\theta_{\bullet})\}/\zeta$$

$$\xi_{11} = \{\zeta_{\pm}(\zeta_{+}/\zeta_{\pm})\sin(2\theta_{+}) + \zeta_{\pm}(1 - \zeta_{+}/\zeta_{\pm})\sin(2\theta_{-}) + \zeta_{\circ}\sin(2\theta_{\circ}) + \zeta_{\bullet}\sin(2\theta_{\bullet})\}/\zeta$$

$$\xi_{12} = \{\zeta_{\pm}(\zeta_{+}/\zeta_{\pm})\sin(4\theta_{+}) + \zeta_{\pm}(1 - \zeta_{+}/\zeta_{\pm})\sin(4\theta_{-}) + \zeta_{\circ}\sin(4\theta_{\circ}) + \zeta_{\bullet}\sin(4\theta_{\bullet})\}/\zeta \quad (11)$$

Elements of the extensionally anisotropic, or extension-shear coupled stiffness matrix ($\mathbf{A}_F$) are related to the lamination parameters by:

$$A_{11} = \{U_1 + \xi_1 U_2 + \xi_2 U_3\} \times H$$

$$A_{12} = A_{21} = \{-\xi_2 U_3 + U_4\} \times H$$

$$A_{22} = \{U_1 - \xi_1 U_2 + \xi_2 U_3\} \times H$$

$$A_{66} = \{-\xi_2 U_3 + U_5\} \times H$$

$$A_{16} = A_{61} = \{\xi_3 U_2/2 + \xi_4 U_3\} \times H$$

$$A_{26} = A_{62} = \{\xi_3 U_2/2 - \xi_4 U_3\} \times H \quad (12)$$

Elements of the bending-twisting coupled stiffness matrix ($\mathbf{D}_F$) are calculated from Eq. (4) or for non-quasi-homogeneous properties:

$$D_{11} = \{U_1 + \xi_9 U_2 + \xi_{10} U_3\} \times H^3/12$$

$$D_{12} = D_{21} = \{U_4 - \xi_{10} U_3\} \times H^3/12$$

$$D_{16} = D_{61} = \{\xi_{11} U_2/2 + \xi_{12} U_3\} \times H^3/12$$

$$D_{22} = \{U_1 - \xi_9 U_2 + \xi_{10} U_3\} \times H^3/12$$

$$D_{26} = D_{62} = \{\xi_{11} U_2/2 - \xi_{12} U_3\} \times H^3/12$$

$$D_{66} = \{-\xi_{10} U_3 + U_5\} \times H^3/12 \quad (13)$$

where the laminate invariants are given in terms of the reduced stiffness properties of Eqs (9) by:

$$U_1 = \{3Q_{11} + 3Q_{22} + 2Q_{12} + 4Q_{66}\}/8$$

$$U_2 = \{Q_{11} - Q_{22}\}/2$$

$$U_3 = \{Q_{11} + Q_{22} - 2Q_{12} - 4Q_{66}\}/8$$

$$U_4 = \{Q_{11} + Q_{22} + 6Q_{12} - 4Q_{66}\}/8$$

$$U_5 = \{Q_{11} + Q_{22} - 2Q_{12} + 4Q_{66}\}/8 \quad (14)$$

IV. The Equivalent Fully Isotropic Laminate

A Fully Isotropic Laminate, or FIL, offers a benchmark stacking sequence configuration, against which all laminates may be compared. However, for thin laminates, with up to 21 plies, these so called benchmark configurations exist only for 18-ply laminates, e.g.

$$[60/-60_2/0_3/60_2/0/-60/60_2/-60_3/0_2/60]_T \tag{15}$$

Additionally, all 18-ply FILs correspond only to $\pi/3$ isotropy, whereby ply orientations have 60° separations, rather than the 45° separations in standard ply orientations, as assumed in this article. This has consequences for the development of failure envelopes for strength comparisons, described later.

To overcome this deficiency, the concept of an Equivalent Fully Isotropic Laminate, with any number of plies or ply angles, may be adopted. The stiffness properties for FIL configuration are now replaced by a set of stiffness properties for the Equivalent FIL, for which no physical stacking sequence configuration exists. The stiffness properties for the Equivalent Fully Isotropic Laminate are readily obtained (Tsai and Hahn 1980) from the laminate invariants of Eqs (14), expressed in terms of their isotropic material counterparts, where $E_1 = E_2$, $\nu_{12} = \nu_{21}$, etc.:

$$E_{Iso} = 2(1 + \nu_{Iso})G_{Iso} = U_1(1 - \nu_{Iso}^2) \tag{16}$$

where

$$\nu_{Iso} = U_4/U_1 \tag{17}$$

and

$$G_{Iso} = U_5 \tag{18}$$

The Young's modulus, E_{Iso}, and Poisson ratio, ν_{Iso}, and shear modulus, G_{Iso}, are the equivalent isotropic material properties of a composite laminate of thickness, H, corresponding to the total number of plies, n, of uniform thickness, t, and from which the equivalent isotropic stiffness properties for laminates with any number of plies then follows:

$$A_{Iso} = A_{11} = A_{22} = E_{Iso}H/(1 - \nu_{Iso}^2) = U_1H \tag{19}$$

$$A_{12} = \nu_{Iso}A_{11} \tag{20}$$

$$A_{66} = U_5H \tag{21}$$

The bending stiffness elements follow from Eq. (4):

$$D_{Iso} = E_{Iso}H^3/(1 - \nu_{Iso}^2)/12 = U_1H^3/12 \tag{22}$$

Equation (22) is also used to normalize the buckling results that follow.

V. Stiffness and Strength properties

A typical IM7/8552 carbon-fiber/epoxy material is adopted, for which the properties are listed in Table 2.

Table 2 - Material properties for Carbon/Epoxy composite

Material properites:		Carbon/Epoxy IM7/8552	
Compressive moduli	E_1	143 GPa	20,740,397 psi
	E_2	9.6 GPa	1,392,362 psi
Shear modulus	G_{12}	5.2 GPa	754,196 psi
Poison's ratio	ν_{12}	0.338	0.338
Density	ρ	1.57 g/cm^3	0.057 lb/in^3
Tensile moduli	E_1	176 GPa	25,526,643 psi
	E_2	8.9 GPa	1,290,836 psi
Compressive strength	σ_1^C	885 MPa	128,358 psi
	σ_2^C	233 MPa	33,794 psi
	τ_{12}^F	56.3 MPa	8,166 psi
Tensile strength	σ_1^T	-2,352 MPa	341,128,774 psi
	σ_2^T	-47 MPa	6,816,774 psi

For a lamina thickness t = 0.1397mm and stacking sequence $[+/-/\bullet_2/\circ/-/\circ/-/\bullet/\circ/+/-/\bullet/+/\bullet/+/-_2/\bullet/\circ]_T$, the non-dimensional parameters described above are verified by the calculations in Table 3, where the first two columns provide the ply number, k, and orientation, θ, respectively. Subsequent columns illustrate the summations, for each ply orientation, of $(z_k - z_{k-1})$, $(z_k^2 - z_{k-1}^2)$ and $(z_k^3 - z_{k-1}^3)$, relating to the **A**, **B** and **D** matrices, respectively. The distance from the laminate mid-plane, z, is expressed in term of ply thickness t, which is assumed to be of unit value.

Table 3 – Calculation procedure for the non-dimensional parameters for an $\mathbf{A_F B_0 D_F}$ laminate: $[+/-/\bullet_2/\circ/-/\circ/-/\bullet/\circ/+/-/\bullet/+/\bullet/+/-_2/\bullet/\circ]_T$.

			A					**B**					**D**				
Ply	θ	$(z_k - z_{k-1})$	$A\Sigma_+$	$A\Sigma_-$	$A\Sigma_\circ$	$A\Sigma_\bullet$	$(z_k^2 - z_{k-1}^2)$	$B\Sigma_+$	$B\Sigma_-$	$B\Sigma_\circ$	$B\Sigma_\bullet$	$(z_k^3 - z_{k-1}^3)$	$D\Sigma_+$	$D\Sigma_-$	$D\Sigma_\circ$	$D\Sigma_\bullet$
			4	6	4	6		0	0	0	0		400	600	400	600
1	+	1	→ 1				-19	→-19				271	→271			
2	–	1	→	1			-17	→	-17			217	→	217		
3	●	1		→		1	-15		→		-15	169		→		169
4	●	1		→		1	-13		→		-13	127		→		127
5	○	1		→	1		-11		→	-11		91		→	91	
6	–	1	→	1			-9	→	-9			61	→	61		
7	○	1		→	1		-7		→	-7		37		→	37	
8	–	1	→	1			-5	→	-5			19	→	19		
9	●	1		→		1	-3		→		-3	7		→		7
10	○	1		→	1		-1		→	-1		1		→	1	
11	+	1	→ 1				1	→ 1				1	→ 1			
12	–	1	→	1			3	→	3			7	→	7		
13	●	1		→		1	5		→		5	19		→		19
14	+	1	→ 1				7	→ 7				37	→ 37			
15	●	1		→		1	9		→		9	61		→		61
16	+	1	→ 1				11	→ 11				91	→ 91			
17	–	1	→	1			13	→	13			127	→	127		
18	–	1	→	1			15	→	15			169	→	169		
19	●	1		→		1	17		→		17	217		→		217
20	○	1		→	1		19		→	19		271		→	271	

The non-dimensional parameters arising from the summations of Table 3 are: n_+ (= ${}_A\Sigma_+$) = 4, n_- = 6, $n_\bigcirc$ = 4 and $n_\bullet$ = 6, and ζ_+ (= 4 × ${}_D\Sigma_+$) = 1600, ζ_- = 2400, $\zeta_\bigcirc$ = 1600 and $\zeta_\bullet$ = 2400, where $n^3 = 20^3 = \zeta = \zeta_+ + \zeta_- + \zeta_\bigcirc + \zeta_\bullet$ = 8000 and $\zeta_\pm = \zeta_+ + \zeta_-$ = 4000. The **B** matrix summations confirm that $B_{ij} = 0$ for this laminate.
For fiber angles θ = ±45° and 0° in place of symbols ± and O respectively, the transformed reduced stiffness properties are given in Table 4, which are readily calculated using Eqs (8).

Table 4 – Transformed reduced stiffness (N/mm^2) for IM7/8552 carbon-fiber/epoxy with θ = -45°, 45°, 0° and 90°.

θ	Q'_{11}	Q'_{12}	Q'_{16}	Q'_{22}	Q'_{26}	Q'_{66}
-45	45,280	34,880	-33,608	45,280	-33,608	36,810
45	45,280	34,880	33,608	45,280	33,608	36,810
0	144,105	3,270	0	9,674	0	5,200
90	9,674	3,270	0	144,105	0	5,200

Equations (5) and (7) yield the final stiffness matrices for laminate: $[+/-/\bullet_2/\bigcirc/-/\bigcirc/-/\bullet/\bigcirc/+/-/\bullet/+/\bullet/+/-_2/\bullet/\bigcirc]_T \equiv [45/-45/90_2/0/-45/0/-45/90/0/45/-45/90/45/90/45/-45_2/90/0]_T$:

$$\begin{bmatrix} A_{11} & A_{12} & A_{16} \\ & A_{22} & A_{26} \\ \text{Sym.} & & A_{66} \end{bmatrix} = \begin{bmatrix} 151{,}891 & 53{,}295 & -9{,}390 \\ & 189{,}451 & -9{,}390 \\ \text{Sym.} & & 58{,}688 \end{bmatrix} \text{N/mm}$$

$$\begin{bmatrix} D_{11} & D_{12} & D_{16} \\ & D_{22} & D_{26} \\ \text{Sym.} & & D_{66} \end{bmatrix} = \begin{bmatrix} 98{,}810 & 34{,}670 & -6{,}109 \\ & 123{,}245 & -6{,}109 \\ \text{Sym.} & & 38{,}179 \end{bmatrix} \text{N.mm}$$

and the quasi-homogeneous nature of this anisotropic laminate is readily verified by Eq. (4).

VI. Laminate Configurations and Lamination Parameter Design Space

Table 5 presents the number of stacking sequence configurations in the definitive list of $\mathbf{A}_F\mathbf{B}_0\mathbf{D}_F$ laminates, with up to 21 plies, and Table 6 presents the corresponding number with quasi-homogeneous anisotropic properties. This class of laminate represents a significant simplification in the laminate design process, given that the bending stiffness follows directly from the extensional stiffness properties, see Eq. (4). In the appendix, Table 9 presents the stacking sequence configurations and non-dimensional parameters for Quasi-Homogeneous Anisotropic Laminates, or QHALs, for each ply number grouping (*n*) in abridged form.

For the purposes of assessing the buckling performance under material strength constraints, QHALs are compared to a non-conforming group of laminates where the constraint between extensional anisotropy and bending anisotropy is relaxed, i.e. $D_{16} \neq A_{16} \times H^2/12$ and $D_{26} \neq A_{26} \times H^2/12$; all other (orthotropic) stiffness elements remain concomitant, as defined in Eq. (4). The number of solutions for each ply number grouping, *n*, for Pseudo-*QHAL*s is reported in Table 7.

Table 5 – Number of laminate stacking sequence configurations with extension-shearing and bending-twisting coupling for each ply number (*n*) grouping.

n	2	3	4	5	6	7	8	9	10	11	12	13	14	15	16	17	18	19	20	21
$\mathbf{A}_F\mathbf{B}_0\mathbf{D}_F$	1	4	3	14	12	66	51	322	242	1,844	1,192	11,652	6,848	83,574	43,831	654,804	319,502	5,733,946	2,584,228	53,588,464

Table 6 – Number of quasi-homogeneous anisotropic laminate (QHAL) stacking sequence configurations for each ply number (n) grouping. These laminate designs possess extension-shearing and bending-twisting coupling and $D_{ij} = A_{ij}H^2/12$.

n	3	4	5	6	7	8	9	10	11	12	13	14	15	16	17	18	19	20	21
$\mathbf{A}_F\mathbf{B}_0\mathbf{D}_F$	1	1	1	1	4	3	1	1	13	3	52	29	48	47	209	82	598	367	381

Table 7 – Number of non-conforming or pseudo quasi-homogeneous anisotropic laminate stacking sequence configurations, for each ply number (n) grouping. These laminate designs are similar to those of Table 6, but whilst the orthotropic elements of the stiffness matrices are quasi-homogeneous, the anisotropic elements are not, i.e. $D_{16} \neq A_{16} \times H^2/12$ and $D_{26} \neq A_{26} \times H^2/12$.

n	3	4	5	6	7	8	9	10	11	12	13	14	15	16	17	18	19	20	21
$\mathbf{A}_F\mathbf{B}_0\mathbf{D}_F$	1	0	3	3	14	4	25	23	97	39	428	325	1,264	622	4,855	3,136	21,188	9,997	55,581

The lamination parameter design spaces for QHOLs and non-conforming quasi-homogeneous anisotropic laminates are illustrated in Figs 3 and 4, respectively.

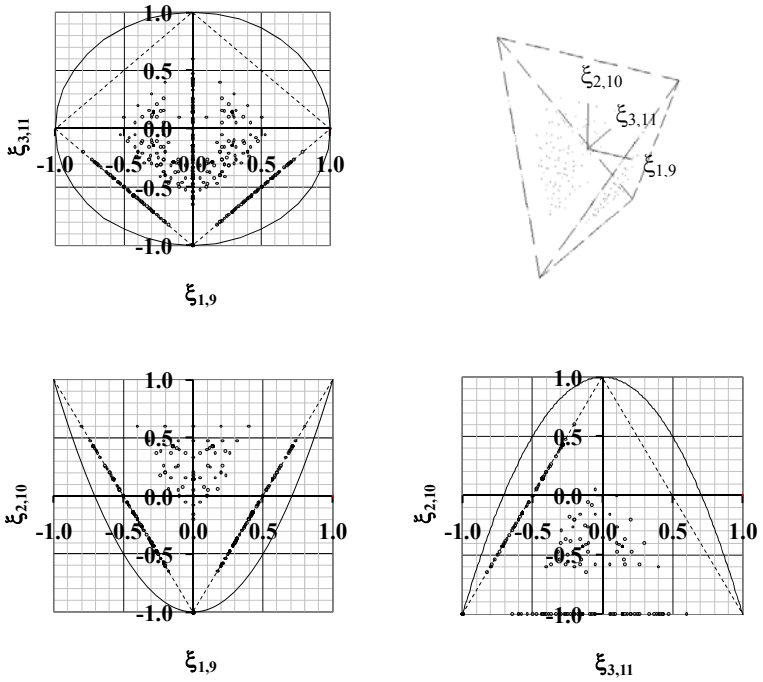

Figure 3 – Third angle projection of the lamination parameter design space for the 1,842 quasi-homogeneous anisotropic laminates with up to 21 plies. Circular and parabolic regions are bounds for laminates with arbitrary ply angle orientations. Standard ply orientations ±45, 0 and 90°, are bounded by *diamond* and *triangular* shaped regions; illustrated as an isometric view.

Standard ply orientations ±45, 0 and 90° are bounded by the *diamond* and *triangular* shaped regions of Fig. 3, but closer inspection of the isometric view reveals that, with the exception of 4 laminates detailed below, 1,838 solutions lie either within the plane of the front triangular face or the plane of the two triangular side faces only.

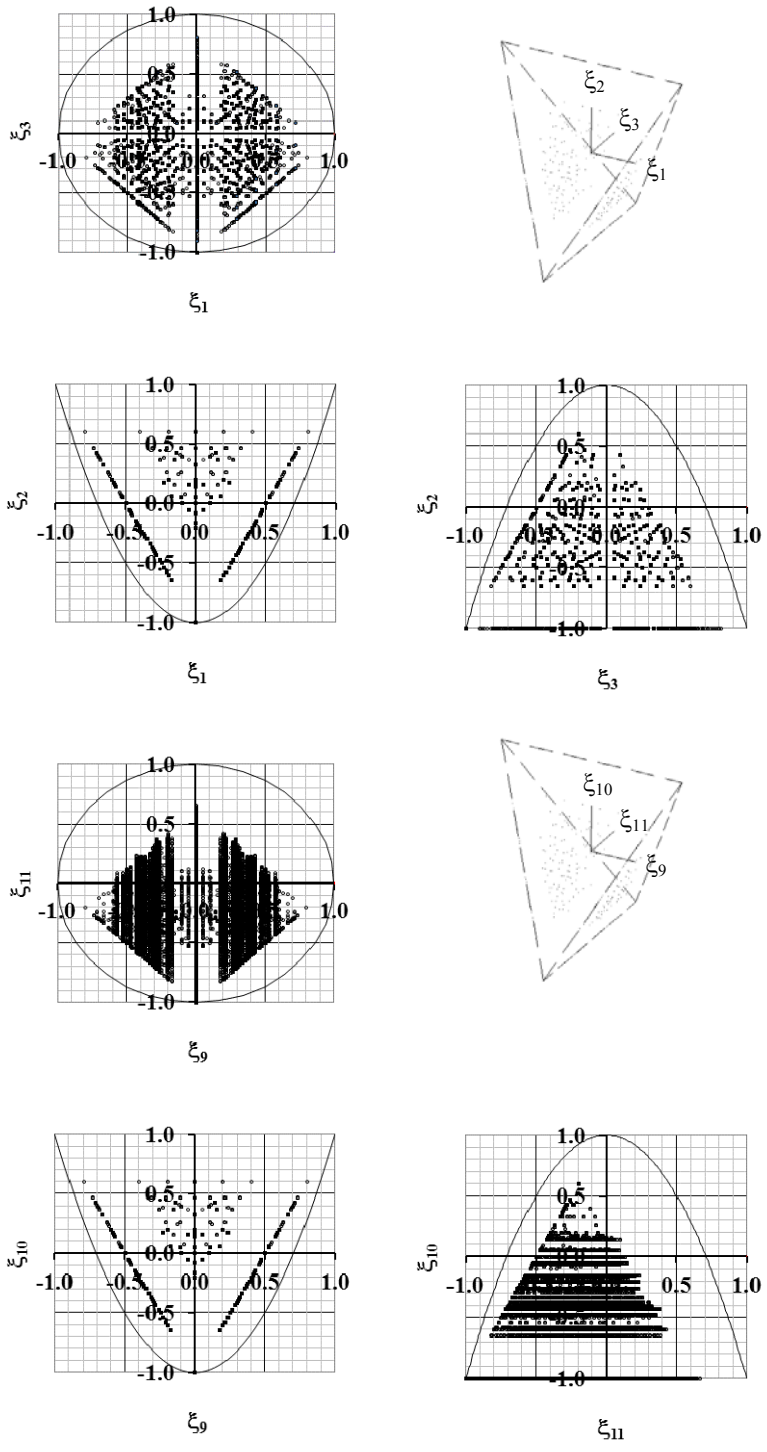

Figure 4 – Third angle projection of the lamination parameter design space for the 99,447 pseudo quasi-homogeneous anisotropic laminates with up to 21 plies. Circular and parabolic regions are bounds for laminates with arbitrary ply angle orientations. Standard ply orientations ±45, 0 and 90°, are bounded by *diamond* and *triangular* shaped regions; illustrated as an isometric projection, repeated from Fig. 3.

Four exceptions are:

$$[45/-45/90/90/0/-45/0/-45/90/0/45/-45/90/45/90/45/-45/-45/90/0]_T$$
$$[45/90/-45/-45/0/90/0/90/-45/0/45/90/-45/45/-45/45/90/90/-45/0]_T$$
$$[45/-45/0/0/90/-45/90/-45/0/90/45/-45/0/45/0/45/-45/-45/0/90]_T$$
$$[45/0/-45/-45/90/0/90/0/-45/90/45/0/-45/45/-45/45/0/0/-45/90]_T$$

and are the only solutions that include all 4 standard ply orientations. Their lamination parameters, $\xi_{1,9}$= -0.1, -0.1, 0.1 and 0.1, respectively, and they share the same lamination parameters $\xi_{2,10} = 0$ and $\xi_{3,11} = 0.1$. A similar discovery was made[4] for Quasi-Homogeneous *Orthotropic* Laminates (QHOLs), in which only a solution exists for laminates with up to 21 plies, i.e. $[45/0/90_2/-45/0/-45/0/90/-45/45/0/90/45/90/45/0_2/90/-45]_T$.

Similarly, of the 99,447 Pseudo-QHAL solutions illustrated on Fig. 4, only 924 include all 4 standard ply orientations, hence the vast majority of the lamination parameters lie on the bounding faces of the design space. Note that only the orthotropic stiffness elements of the Pseudo-QHAL solutions are concomitant, hence the design spaces representing the extensional and bending stiffness properties are identical only on one ($\xi_{1,9}$, $\xi_{2,10}$) plane.

Six groups of 18-ply QHALs from Table 6 and their comparators from Table 7 are used for the comparisons that follow. These were selected on the basis of the non-dimensional parameters, accounting for different combinations of ply orientations and for the most extreme cases of anisotropy. The stacking sequences for each group are listed in Table 10 in the appendix, the corresponding non-dimensional parameters are listed in Table 11 and stiffness matrices for each QHAL are given in Table 12; derived from the material properties listed in Table 2. The Pseudo-QHAL comparators share identical orthotropic stiffness properties to their QHAL counterparts, therefore only differences in the anisotropic stiffness properties are identified in Table 12.

VII. Design of laminated anisogrid panels

Computer Modeling

The analysis involves an exact, infinite strip approach, in the sense that it is based on the exact solution of the classical thin plate differential equations but while longitudinal plate boundaries (or edges) are modelled exactly, the transverse boundaries are closely approximated by the use of a sufficient number of point constraints. These point constraints, forming the rigid supports described in the previous section, are introduced by the method of Lagrangian multipliers, whereby compatible wavelengths are coupled to achieve a predefined pattern of node points, i.e. points of enforced zero displacement. These node points repeat at intervals of the panel length *a*, see Fig. 5(a), since the analysis accounts for an infinitely long plate, thus forming a series of plates joined end to end. The rigid supports, arranged to form skew supports in previous work, are shown here as a hexagonal support pattern. To form an array of hexagonal supports this pattern must also repeat in the transverse direction, but to avoid incompatible arrangement of supports in adjacent bays, as illustrated in Fig. 5(b), a phase shift correction, χ, must be introduced as demonstrated in Fig. 5(c). With few geometric exceptions, the new buckling predictions that follow are only possible through this enhancement to existing theory[8] and the associated computer programVICONOPT[9], to allow for plate assemblies that are continuous over supports at regular longitudinal and transverse intervals, such that the transverse supports are correctly orienated across adjacent bays at skew angle α, see Fig. 5(c).

Laminate Design

This section explores whether design guidelines can be developed for non-standard geometries and whether concomitant laminate properties offer any form of optimal solution when the design envelope extends across a wide range of combined load cases, when strength constraints are active. Strength constraints are represented by Tsai-Wu failure criteria, corresponding to:

$$F_1\sigma_1 + F_2\sigma_2 + F_{11}\sigma_1^2 + F_{22}\sigma_2^2 + F_{66}\tau_{12}^2 - (F_{11}F_{22})^{½}\,\sigma_1\sigma_1 = 1 \qquad (23)$$

Individual terms were derived from the strength constraint data listed in Table 2 as follows:

$$F_1 = (1/\sigma_1^T + 1/\sigma_1^C) = 704.773 \times 10^{-6}\ \text{mm}^2/\text{N}$$
$$F_2 = (1/\sigma_2^T + 1/\sigma_2^C) = -16{,}984.750 \times 10^{-6}\ \text{mm}^2/\text{N}$$
$$F_{11} = -1/\sigma_1^T\sigma_1^C = 0.480 \times 10^{-6}\ (\text{mm}^2/\text{N})^2$$
$$F_{22} = -1/\sigma_2^T\sigma_2^C = 91.316 \times 10^{-6}\ (\text{mm}^2/\text{N})^2$$
$$F_{66} = (1/\tau_{12}^F)^2 = 315.488 \times 10^{-6}\ (\text{mm}^2/\text{N})^2$$

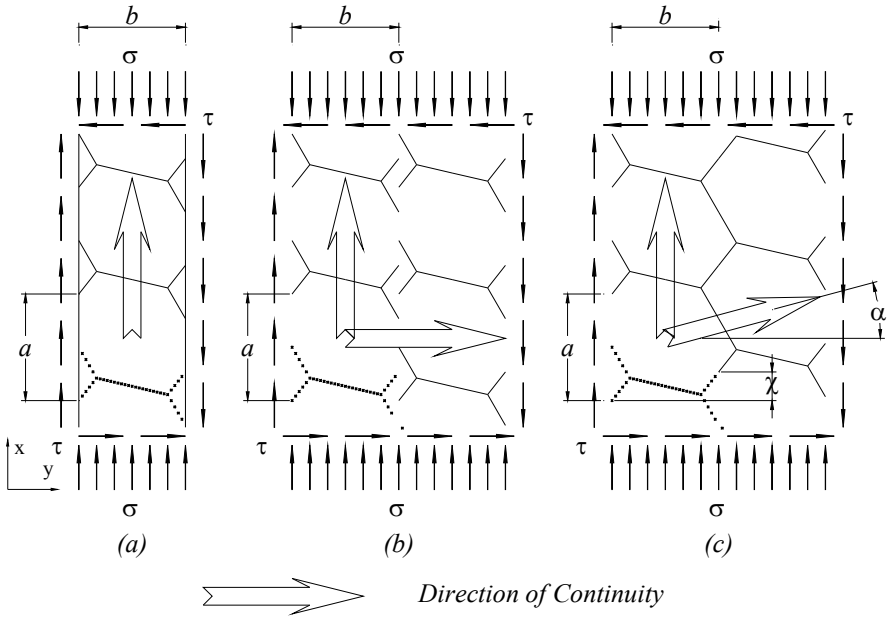

Figure 5 - Support conditions and positive stress directions for hexagonal plate (*after Ref. 3*): (a) with uniaxial continuity, whereby boundary conditions are enforced by the Lagrangian multiplier method, i.e. discrete point constraints repeat at bay length intervals, *a*; (b) array with biaxial (transverse) continuity, enforced by recurrence equations, i.e. transverse mode repeats at bay width intervals, *b* and (c) array with skew-transverse continuity, which is as (b) but with phase shift χ in the adjacent bay.

Optimized laminate configurations were to be obtained using VICONOPT, incorporating a new sizing strategy based on lamination parameter, for comparison with the design spaces of Figs 3 and 4. However, at the time of writing, strength constraints were not incorporated into the sizing strategy and therefore only a limited number of optimized results are presented using this strategy, whereby all start designs were based on an 18-ply Fully Isotropic Laminate, or FIL, on a rectangular (a/b = 1.15) array of supports, with bay width, *b*, optimized such that the buckling and strength constraint were coincident under pure shear loading. The Tsai-Wu failure envelope, calculated over a broad range of shear and compression load combinations, became the load set against which the buckling constraints were to be optimized. A surrogate set of ply orientations, based on standard ply orientations +45, -45, 0 and 90°, were used overcome the constraint that the 18-ply FIL has non-standard ply orientations +60, -60 and 0°. The 18-ply FIL is used to generate the laminate stiffness matrix from which the strains are calculated from each load combinations. The ply level stresses are however calculated for the surrogate set of standard ply orientations with identical material properties and ply thickness to the 18-ply FIL. Each load combination was then adjusted monotonically until the strength constraint, defined by Eq. (23) was reached. This surrogate procedure was validated against 72-ply $\pi/3$ and $\pi/4$ fully isotropic laminates: $[60/\text{-}60_2/0_3/60_2/0/\text{-}60/60_2/\text{-}60_3/0_2/60]_{4T}$ and; $[45/\text{-}45/0/90/0/90/\text{-}45/90/45/0/45/\text{-}45/45/\text{-}45/90/\text{-}45/0/45/0/90/0/90/45/\text{-}45]_{3T}$.

A baseline analysis of the 18-ply FIL laminate with a range of supporting geometries is presented in Fig. 6. In previous work[3], plate thickness was adjusted in the isotropic case to maintain constant panel mass, based on the relative densities of aluminum and composite laminate materials respectively. The ratio of buckling load and non-dimensional buckling factor for the two materials were thus the same, allowing direct comparison between the buckling strength/weight ratio of composite and metallic panel array structures. In the present work, results are normalized against the equivalent fully isotropic laminate, hence no material property adjustments are required and the comparisons are therefore literally like with like.

A standard VICONOPT optimization for pure shear loading was performed in which the ply thickness was the design variable so that a minimum mass solution, subject to strength constraints could be established, see Table 8. Here the rectangular panel, with an applied shear load corresponding to the buckling load and material strength constraint of the 18-ply $\pi/3$ FIL, therefore has a small material strength reserve and the optimization is driven by the buckling constraint. The optimized skew plate result was virtually identical to the rectangular plate result given that the buckling reserve could not be exploited without violating the material strength constraint.

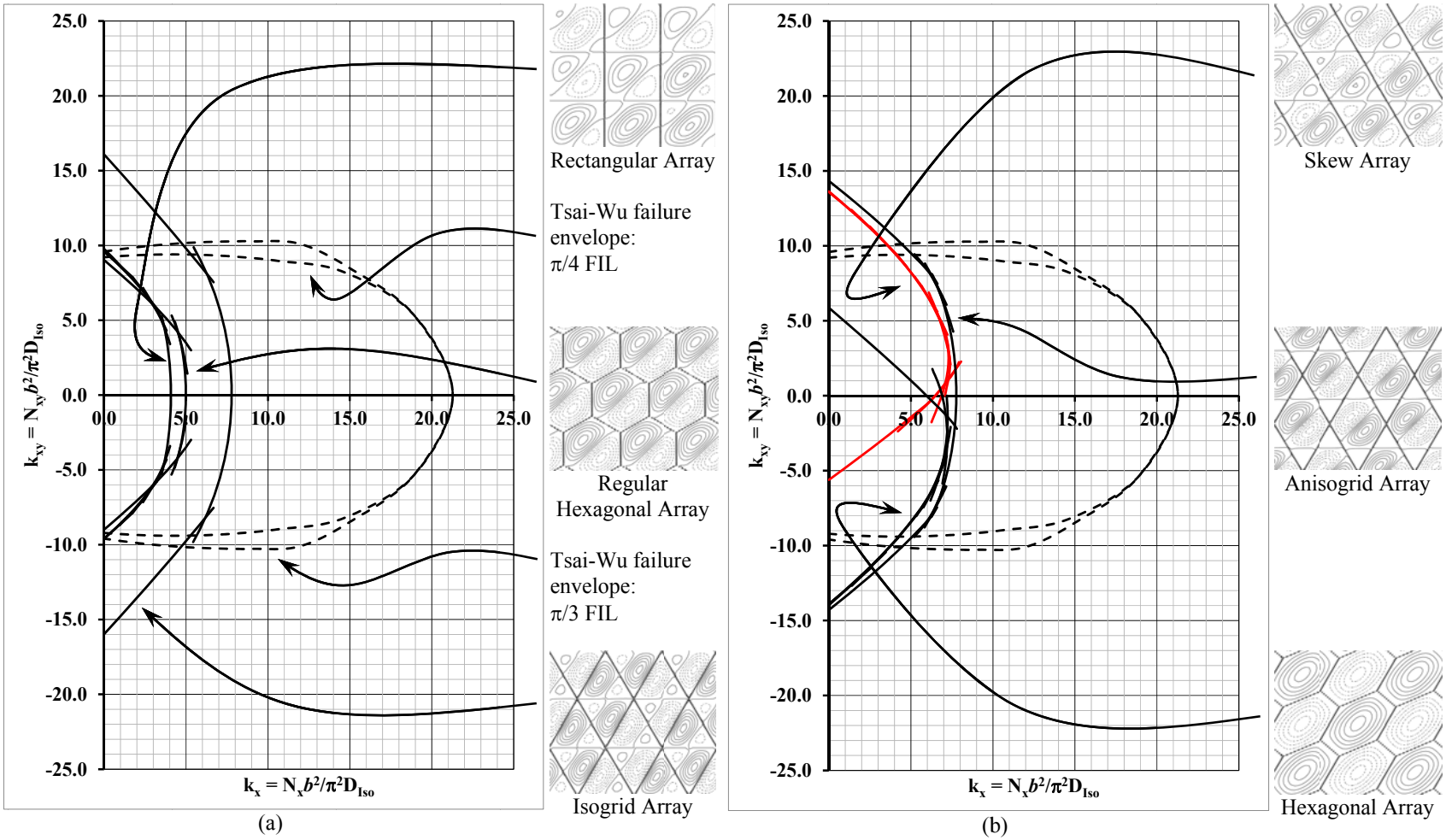

(a) (b)

Figure 6 – Buckling factor envelopes for 18-ply Fully Isotropic Laminates, or FILs, with: (a) rectangular, regular hexagonal and isogrid plate arrays and (b) skew (30°), anisogrid and hexagonal plate arrays. Superimposed are the Tsai-Wu failure envelopes corresponding to the fully isotropic laminate with standard (π/4) and non-standard (π/3) ply orientations. Buckling modes for each planform geometry correspond to pure positive shear loading.

Table 8 – VICONOPT sizing strategy results for rectangular, hexagonal and skew plate arrays. The common plate length, a = 459.85 mm (6.29 in.) and width, b = 139 mm (5.47 in.). The initial ply thickness, t = 0.1397 mm (0.0055 in.).

1. VICONOPT Original Design Optimization, with strength constraints.				
Geometry:	Regular Hexagonal	Rectangular	30° Skew	
Shear load direction:	−ve	−ve	−ve	+ve
Governing constraint:	*Buckling*	*Buckling*	*Buckling*	*Strength*
t	0.1408	0.1378	0.1647	0.1341
$H = n \times t$	2.5344	2.4804	2.9646	2.4138
$n_{\text{Equivalent}}$	18.14	17.76	21.22	17.28
n_{Rounded}	18	18	22	18
2. VICONOPT Lamination Parameter Optimization, without strength constraints.				
$H = n \times t$	2.53	2.42	2.87	2.18
$n_{\text{Equivalent}}$	18.09	17.34	20.53	15.59
n_{Rounded}	18	18	20	16
Target (ξ_1, ξ_2, ξ_3)	(-0.15, -0.09, 0.10)	(-0.21, -0.01, -0.11)	(0.20, 0.20, 0.00)	(-0.01, 0.03, 0.03)
Target (ξ_9, ξ_{10}, ξ_{11})	(-0.12, -0.21, -0.03)	(-0.25, -0.35, -0.01)	(-0.18, -0.19, 0.00)	(0.03, -0.03, -0.02)
3. Stacking Sequence Optimization*				
Actual (ξ_1, ξ_2, ξ_3)	-0.22, -0.11, 0.11	-0.22, -0.11, 0.00	0.20, 0.20, 0.00	0.00, 0.00, 0.00
Actual (ξ_9, ξ_{10}, ξ_{11})	-0.14, -0.22, -0.02	-0.27, -0.35, 0.29	-0.18, -0.21, 0.00	0.04, -0.02, -0.02
4. VICONOPT Final Analysis Check				
Buckling load factor	0.985	1.101	0.925	1.034
$(n_{\text{Equivalent}}/n_{\text{Rounded}})^3$	0.985	1.119	0.925	1.081

***Final stacking sequences:**

Regular Hexagonal $\mathbf{A}_F\mathbf{B}_0\mathbf{D}_F$: $[45/-45/90/0/-45/90/45/45/90/90/90/45/45/-45/0/45/-45/90]_T$

Rectangle $\mathbf{A}_F\mathbf{B}_0\mathbf{D}_F$: $[-45/45/90/90/45/-45/0/-45/90/90/-45/0/45/-45/90/90/-45/45]_T$

Skew$^{(\text{-ve shear})}$ $\mathbf{A}_S\mathbf{B}_0\mathbf{D}_S$: $[90/-45/45/45/-45/0/0/90/0/0/0/0/90/90/0/0/45/-45/-45/45/90]_T$

Skew$^{(\text{+ve shear})}$ $\mathbf{A}_I\mathbf{B}_0\mathbf{D}_F$: $[45/-45/0/90/90/-45/0/0/45/90/45/-45/45/-45/90/0]_T$

A VICONOPT lamination parameter optimization was performed as a 2nd step, using the same start designs as the 1st step, but omitting the strength constraints; the 18-ply FIL start design has lamination parameters (ξ_1, ξ_2, ξ_3) = (ξ_9, ξ_{10}, ξ_{11}) = (0, 0, 0). All lamination parameters were free to develop independently, but the final design and resulting stacking sequences demonstrate that without material strength constraints the in-plane stiffness properties are not modified significantly during the optimization. Following the stacking sequence optimization[10] of the 3rd step, a VICONOPT final analysis check showed that any failure to achieve the required critical buckling load was due to the rounding of the plate thickness (i.e. from $n_{\text{Equivalent}}$ to n_{Rounded} plies), rather than a lack of fit to the required lamination parameters. The skew geometry produced a fully uncoupled laminate design solution when subjected to pure negative shear load, whereas positive shear produced a quasi-isotropic solution; with bending-twisting coupling. These results suggest that strength constraints must be active in order to assess the likelihood of an optimal QHAL solution. Attention is therefore turned to one of the six groups of 18-ply QHALs from Table 10.

Figure 7 illustrates the buckling interaction curves and associated Tsai-Wu failure envelopes for the first of the six comparator groups in Table 10. All three laminate designs have identical extensional stiffness properties, see Table 12, hence the Tsai-Wu failure envelopes are also identical. With the exception of bending-twisting coupling terms, D_{16} (= D_{26}), the Pseudo-QHAL comparators, i.e. laminates 26 and 237, are identical to the QHAL, i.e. laminate 189. The influence of bending-twisting coupling on the buckling envelope is therefore clear from the three comparators. The buckling envelopes for the skew and isogrid plate arrays closely match the Tsai-Wu failure envelope across a broad range of load combinations. However, this is not a common feature for other groups in Table 10. Indeed QHALs only have the potential to influence the design where the buckling and material strength constraints are coincident. Where strength constraints are inactive, as in the case of the Rectangular and Regular Hexagonal arrays in Fig. 7, the extensional properties have little influence and therefore quasi-homogeneous properties have no particular relevance. An optimum solution therefore relies on the ability to match both buckling and material strength constraint envelopes over the range of load combinations of interest.

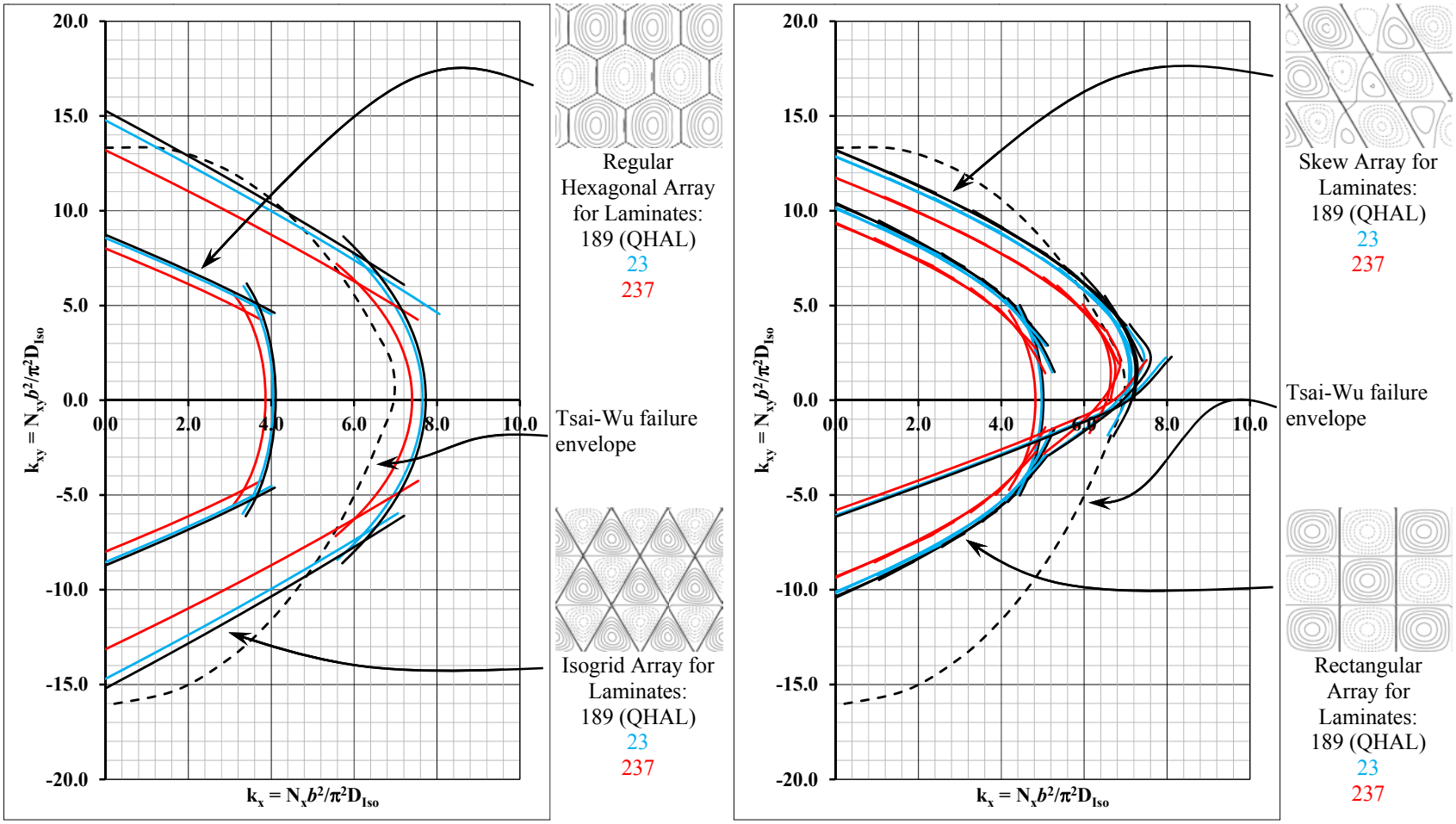

(a) (b)

Figure 7 – Buckling factor envelopes for 18-ply Quasi-Homogeneous Anisotropic Laminate 189, or QHAL, together with Pseudo-QHAL comparators 23 and 237 from Table 10 with: (a) regular hexagonal and isogrid plate arrays and (b) rectangular and skew (30°) plate arrays. Superimposed is the Tsai-Wu failure envelope; identical for all three laminates. Buckling modes for each planform geometry correspond to pure compression loading.

VIII. Concluding Remarks

Quasi-Homogeneous Anisotropic Laminates or QHALs have been described as having identical anisotropy with respect to both extension and bending, providing maximum (and minimum) in-plane and out-of-plane reinforcement in the same direction, and thus providing a minimum mass solution. However, this implies matching buckling and strength constraint envelopes. Where strength constraints are inactive, the extensional properties of the laminate have little influence on the design and therefore quasi-homogeneous properties have no particular relevance. An optimum QHAL solution relies on the ability to match both buckling and material strength constraint envelopes over the range of load combinations of interest. However, concomitant extensional and bending stiffness properties are not a necessary requirement for achieving this.

Acknowledgements.

The Royal Aeronautical Society is gratefully acknowledged for the Aerospace Speaker's Travel Award that supported the 1st author.

References

[1]Wu, K., M. and Avery, B. L. "Fully isotropic laminates and quasi-homogeneous anisotropic laminates," Journal of Composite Materials, Vol. 26, No. 14, 1992, pp. 2107-2117.

[2]York, C. B. "Buckling interaction in regular arrays of distorted hexagonal plates," *Aeronautical J.,* Vol. 107, No. 1074, 2003, pp. 461-468.

[3]York, C. B. "Buckling interaction in regular arrays of rigidly supported composite laminated plates with orthogrid, isogrid and anisogrid planform," *AHS J.* Vol. 52, No. 4, 2007, pp. 343-359.

[4]York C. B. "A unified approach to the characterization of coupled composite laminates: Benchmark configurations and special Cases," *J. Aero. Eng., ASCE*, Vol. 23, No. 4, 2010, pp. 1-24.

[5]Engineering Sciences Data Unit, "Stiffnesses of laminated plates", ESDU Item No. 94003, 1994.

[6]York, C. B. "On composite laminates with extensional-anisotropy", *Proc. 49th AIAA/ASME/ASCE/AHS/ASC Structures, Structural Dynamics, and Materials Conf.*, Paper No. AIAA-2008-1752, Schaumburg, Illinois, 2008.

[7]York, C. B. "Characterization of non-symmetric forms of fully orthotropic laminates," *AIAA Journal of Aircraft*, Vol. 46, No. 4, 2009, pp. 1114-25.

[8]York, C. B. and Williams, F. W. "Theory and buckling results for infinitely wide, stiffened skew plate assemblies," *Composite Structures*, Vol. 28, No. 2, 1994, pp.189-200.

[9]Williams, F. W., Kennedy, D., Butler, R. and Anderson, M. S., "VICONOPT: program for exact vibration and buckling analysis or design of prismatic plate assemblies", *AIAA Journal*, Vol. 29, No. 11, 1991, pp. 1927-1928.

[10]Kennedy, D., Park, B and Unsworth, M. D. "Towards Global Layup Optimisation of Composite Panels with Initial Buckling Constraints," *Proc. 8th ASMO UK/ISSMO Conf.*, London, UK, 2010, pp. 221-231.

Appendix

Table 9 – $\mathbf{A}_F\mathbf{B}_0\mathbf{D}_F$ Quasi-Homogeneous Anisotropic Laminate (*QHAL*) stacking sequences and associated non-dimensional parameters. Standard ply orientations 45, -45, 0 and 90°, are represented in this study in place of symbols +, −, ○ and ●, respectively.

Ref.		Sequence	n	$n_{\pm}$	$n_{○}$	$n_{●}$	ζ	$\zeta_{\pm}$	$\zeta_{○}$	$\zeta_{●}$	n_{+}	ζ_{+}
QHAL	1	+ + +	3	3	0	0	27	27	0	0	3.0	0.0
QHAL	2	+ + + +	4	4	0	0	64	64	0	0	4.0	0.0
QHAL	3	+ + + + +	5	5	0	0	125	125	0	0	5.0	0.0
QHAL	4	+ − + + + +	6	6	0	0	216	216	0	0	6.0	0.0
QHAL	5	+ ○ + + ○ +	7	5	2	0	343	245	98	0	5.0	0.0
QHAL	6	+ − + + − +	7	7	0	0	343	343	0	0	5.0	98.0
QHAL	7	+ ● + + ● +	7	5	0	2	343	245	0	98	5.0	0.0
QHAL	8	+ + + + + +	7	7	0	0	343	343	0	0	7.0	0.0
QHAL	9	+ ○ ○ + + ○	8	4	4	0	512	256	256	0	4.0	0.0
QHAL	10	+ ● ● + + ●	8	4	0	4	512	256	0	256	4.0	0.0
QHAL	11	+ + + + + + +	8	8	0	0	512	512	0	0	8.0	0.0
QHAL	12	+ + + + + + + +	9	9	0	0	729	729	0	0	9.0	0.0
QHAL	13	+ + + + + + + + +	10	10	0	0	1000	1000	0	0	10.0	0.0
QHAL	14	+ ○ + ○ + + ○ + ○ +	11	7	4	0	1331	847	484	0	7.0	0.0
	:		:									
QHAL	26	+ + + + + + + + + +	11	11	0	0	1331	1331	0	0	11.0	0.0
QHAL	27	+ ○ + ○ ○ ○ + + + ○ + ○	12	6	6	0	1728	864	864	0	6.0	0.0
QHAL	28	+ ● + ● ● ● + + + ● + ●	12	6	0	6	1728	864	0	864	6.0	0.0
QHAL	29	+ + + + + + + + + + + +	12	12	0	0	1728	1728	0	0	12.0	0.0
QHAL	30	+ ○ + + + + + ○ + + ○ + +	13	10	3	0	2197	1690	507	0	10.0	0.0
	:		:									
QHAL	81	+ + + + + + + + + + + + +	13	13	0	0	2197	2197	0	0	13.0	0.0
QHAL	82	+ + ○ ○ + + + + + ○ ○ + +	14	10	4	0	2744	1960	784	0	10.0	0.0
	:		:									
QHAL	110	+ + + + + + + + + + + + + +	14	14	0	0	2744	2744	0	0	14.0	0.0
QHAL	111	+ ○ + + + + + + ○ + + ○ + + +	15	12	3	0	3375	2700	675	0	12.0	0.0
	:		:									
QHAL	158	+ + + + + + + + + + + + + + +	15	15	0	0	3375	3375	0	0	15.0	0.0
QHAL	159	+ + ○ + ○ + + + + + ○ + ○ + +	16	12	4	0	4096	3072	1024	0	12.0	0.0
	:		:									
QHAL	205	+ + + + + + + + + + + + + + + +	16	16	0	0	4096	4096	0	0	16.0	0.0

QHAL	206			+	+	O	+	+	+	+	+		O		+	+	+	+	+	O	+	+			17	14	3	0	4913	4046	867	0	14.0	0.0
	:																								:														
QHAL	414			+	+	+	+	+	+	+	+		+		+	+	+	+	+	+	+	+			17	17	0	0	4913	4913	0	0	17.0	0.0
QHAL	415			+	−	−	−	−	−	+	+	−		−	+	+	−	−	−	−	−	+			18	12	6	0	5832	3888	1944	0	12	0
	:																								:														
QHAL	496			+	O	O	+	O	O	O	O	O		O	+	+	O	+	+	O	O	O			18	18	0	0	5832	5832	0	0	18.0	0.0
QHAL	497		+	O	+	+	+	+	+	O	+		+		+	+	+	O	+	O	+	+	+		19	15	4	0	6859	5415	1444	0	15.0	0.0
	:																								:														
QHAL	1094		+	+	+	+	+	+	+	+	+		+		+	+	+	+	+	+	+	+			19	19	0	0	6859	6859	0	0	19.0	0.0
QHAL	1095		+	O	+	O	+	+	+	+	+	O		+	+	+	O	+	O	O	+	+	+		20	14	6	0	8000	5600	2400	0	14.0	0.0
	:																								:														
QHAL	1461		+	+	+	+	+	+	+	+	+	+		+	+	+	+	+	+	+	+	+	+		20	20	0	0	8000	8000	0	0	20.0	0.0
QHAL	1462	+	O	+	O	+	+	+	+	+	+		O		+	+	+	O	O	+	O	+	+	+	21	15	6	0	9261	6615	2646	0	15.0	0.0
	:																								:														
QHAL	1842	+	+	+	+	+	+	+	+	+	+		+		+	+	+	+	+	+	+	+	+	+	21	21	0	0	9261	9261	0	0	21.0	0.0

Table 10 – Stacking sequences for 6 groups of QHAL and Pseudo-QHAL comparators.

Group	*Ref.*	Stacking sequence
	26	$[+/+/+/-/-/-/-/-/-/-/-/-/-/-/+/+/+]_T$
1	*QHAL-189*	$[+/-/-/-/-/-/+/+/-/-/+/+/-/-/-/-/-/+]_T$
	237	$[+/-/-/-/-/-/-/-/+/+/+/+/-/+/-/-/-/-]_T$
	1752	$[+/+/+/+/+/+/-/-/-/-/-/-/+/+/+/+/+/+]_T$
2	*QHAL-2062*	$[+/-/-/+/+/+/+/+/+/-/+/+/-/-/-/+/+/+]_T$
	2215	$[+/-/-/-/+/+/+/+/+/+/+/+/-/+/+/+/-/-]_T$
	2739	$[+/●/●/●/●/●/-/-/●/●/-/-/●/●/●/●/●/+]_T$
3	*2746*	$[+/●/●/-/●/●/●/●/●/●/+/+/●/+/-/●/●/●]_T$
	QHAL-2747	$[+/●/●/+/●/●/●/●/●/●/+/+/●/+/+/●/●/●]_T$
	2753	$[+/-/-/○/○/○/-/-/○/-/-/-/-/-/-/○/○/+]_T$
4	*3149*	$[+/-/+/○/○/+/○/○/+/+/+/+/+/+/○/+/-/○]_T$
	QHAL-3150	$[+/○/○/+/+/+/+/+/+/○/+/+/○/○/○/+/+/+]_T$
	3165	$[+/●/●/○/○/○/-/-/○/●/-/-/●/●/●/○/○/+]_T$
5	*3186*	$[+/●/○/-/●/○/○/○/●/●/+/+/●/+/-/○/○/●]_T$
	QHAL-3187	$[+/●/●/○/○/○/+/+/○/●/+/+/●/●/●/○/○/+]_T$
	3205	$[+/○/○/○/○/○/-/-/○/○/-/-/○/○/○/○/○/+]_T$
6	*3212*	$[+/○/○/-/○/○/○/○/○/○/+/+/○/+/-/○/○/○]_T$
	QHAL-3213	$[+/○/○/○/○/○/+/+/○/○/+/+/○/○/○/○/○/+]_T$

Table 11 – Non-dimensional parameters for 6 groups of QHAL and Pseudo-QHAL comparators corresponding to the stacking sequences listed in Table 10.

Group	*Ref.*	n	$n_{\pm}$	$n_{\circ}$	$n_{\bullet}$	ζ	$\zeta_{\pm}$	ζ_{0}	$\zeta_{\bullet}$	n_{+}	ζ_{+}
	26	18	18	0	0	5832	5832	0	0	6	1728
1	*QHAL-189*	18	18	0	0	5832	5832	0	0	6	3888
	237	18	18	0	0	5832	5832	0	0	6	4608
	1752	18	18	0	0	5832	5832	0	0	12	216
2	*QHAL-2062*	18	18	0	0	5832	5832	0	0	12	1944
	2215	18	18	0	0	5832	5832	0	0	12	3240
	2739	18	6	0	12	5832	1944	0	3888	2	208
3	*2746*	18	6	0	12	5832	1944	0	3888	4	728
	QHAL-2747	18	6	0	12	5832	1944	0	3888	6	0
	2753	18	12	6	0	5832	3888	1944	0	2	2152
4	*3149*	18	12	6	0	5832	3888	1944	0	10	1352
	QHAL-3150	18	12	6	0	5832	3888	1944	0	12	0
	3165	18	6	6	6	5832	1944	1944	1944	2	208
5	*3186*	18	6	6	6	5832	1944	1944	1944	4	728
	QHAL-3187	18	6	6	6	5832	1944	1944	1944	6	0
	3205	18	6	12	0	5832	1944	3888	0	2	208
6	*3212*	18	6	12	0	5832	1944	3888	0	4	728
	QHAL-3213	18	6	12	0	5832	1944	3888	0	6	0

Table 12 – Stiffness matrices for 6 groups of QHAL and Pseudo-QHAL comparators corresponding to the stacking sequences listed in Table 10. The anisotropic elements $A_{16} = A_{26}$ and/or $D_{16} = D_{26}$ are highlighted only where the comparator differs from the QHAL.

Group	[**A**],[**D**] matrices	*Ref.*	Comments
1	$\begin{bmatrix} 113{,}861 & 87{,}709 & -28{,}170 \\ & 113{,}861 & -28{,}170 \\ \text{Sym.} & & 92{,}562 \end{bmatrix}, \begin{bmatrix} 59{,}997 & 46{,}217 & -14{,}844 \\ & 59{,}997 & -14{,}844 \\ \text{Sym.} & & 48{,}774 \end{bmatrix}$	*26* *QHAL-189* *237*	$D_{16} = D_{26} = 18{,}142$ $D_{ij} = A_{ij}H^2/12$ $D_{16} = D_{26} = -25{,}839$
2	$\begin{bmatrix} 113{,}861 & 87{,}709 & 28{,}170 \\ & 113{,}861 & 28{,}170 \\ \text{Sym.} & & 92{,}562 \end{bmatrix}, \begin{bmatrix} 59{,}997 & 46{,}217 & 14{,}844 \\ & 59{,}997 & 14{,}844 \\ \text{Sym.} & & 48{,}774 \end{bmatrix}$	*1752* *QHAL-2062* *2215*	$D_{16} = D_{26} = 41{,}233$ $D_{ij} = A_{ij}H^2/12$ $D_{16} = D_{26} = -4{,}948$
3	$\begin{bmatrix} 54{,}171 & 34{,}718 & 28{,}170 \\ & 279{,}532 & 28{,}170 \\ \text{Sym.} & & 39{,}571 \end{bmatrix}, \begin{bmatrix} 28{,}545 & 18{,}294 & 14{,}844 \\ & 147{,}295 & 14{,}844 \\ \text{Sym.} & & 20{,}852 \end{bmatrix}$	*2739* *2746* *QHAL-2747*	$A_{16} = A_{26} = -9{,}390$; $D_{16} = D_{26} = 11{,}667$ $A_{16} = A_{26} = 9{,}390$; $D_{16} = D_{26} = 3{,}726$ $D_{ij} = A_{ij}H^2/12$
4	$\begin{bmatrix} 196{,}696 & 61{,}213 & 56{,}340 \\ & 84{,}016 & 56{,}340 \\ \text{Sym.} & & 66{,}067 \end{bmatrix}, \begin{bmatrix} 103{,}646 & 32{,}255 & 29{,}688 \\ & 44{,}271 & 29{,}688 \\ \text{Sym.} & & 34{,}813 \end{bmatrix}$	*2753* *3149* *QHAL-3150*	$A_{16} = A_{26} = -37{,}560$; $D_{16} = D_{26} = -3{,}176$ $A_{16} = A_{26} = 37{,}560$; $D_{16} = D_{26} = 9{,}041$ $D_{ij} = A_{ij}H^2/12$
5	$\begin{bmatrix} 166{,}851 & 34{,}718 & 28{,}170 \\ & 166{,}851 & 28{,}170 \\ \text{Sym.} & & 39{,}571 \end{bmatrix}, \begin{bmatrix} 87{,}920 & 18{,}294 & 14{,}844 \\ & 87{,}920 & 14{,}844 \\ \text{Sym.} & & 20{,}852 \end{bmatrix}$	*3165* *3186* *QHAL-3187*	$A_{16} = A_{26} = -9{,}390$; $D_{16} = D_{26} = -11{,}667$ $A_{16} = A_{26} = 9{,}390$; $D_{16} = D_{26} = 3{,}726$ $D_{ij} = A_{ij}H^2/12$
6	$\begin{bmatrix} 279{,}532 & 34{,}718 & 28{,}170 \\ & 54{,}171 & 28{,}170 \\ \text{Sym.} & & 39{,}571 \end{bmatrix}, \begin{bmatrix} 147{,}294 & 18{,}294 & 14{,}844 \\ & 28{,}545 & 14{,}844 \\ \text{Sym.} & & 20{,}852 \end{bmatrix}$	*3205* *3212* *QHAL-3213*	$A_{16} = A_{26} = -9{,}390$; $D_{16} = D_{26} = -11{,}667$ $A_{16} = A_{26} = 9{,}390$; $D_{16} = D_{26} = 3{,}726$ $D_{ij} = A_{ij}H^2/12$